Homo- and Heterometallic Mono-, Di-, and Trinuclear Co^{2+}, Ni^{2+}, Cu^{2+}, and Zn^{2+} Complexes of the "Heteroscorpionate" Ligand (2-Hydroxyphenyl)bis(pyrazolyl)methane and Its Derivatives

Timothy C. Higgs, Norman S. Dean, and Carl J. Carrano*

Department of Chemistry, Southwest Texas State University, San Marcos, Texas 78666

Received September 10, 1997

^{1}H NMR spectra on the paramagnetic Co^{II} and Ni^{II}, ML_2 "sandwich" complexes of the "heteroscorpionate" ligands (2-hydroxyphenyl)bis (pyrazolyl)methane and its derivatives revealed the presence of isomeric, cis ↔ trans equilibria of these complexes in solution. The presence of some of the cis isomer in solution at equilibrium has been exploited to synthesize new heterometallic trinuclear species of the type $[M1(L1O)_2M2(L1O)_2M1][BF_4]$, where M1 (octahedral) and M2 (tetrahedral) are Zn^{2+}, Cu^{2+}, Ni^{2+}, and Co^{2+}. Rearrangements during the synthesis of some of these heterometallic species provided an interesting experimental confirmation of the site preferences (octahedral vs tetrahedral) for the first-row transition metals as predicted on the basis of crystal field stabilization energies. X-ray crystallographic characterization of many of the complexes reported in this study gives the following structural parameters: $[Co_2(L2O)_2Cl_2]\cdot MeCN$, $C_{36}H_{41}N_9Cl_2Co_2O_2$, monoclinic, $a = 10.742(1)$ Å, $b = 21.387(2)$ Å, $c = 16.890(2)$ Å, $\beta = 95.506(8)°$, space group $P2_1/c$, $Z = 4$; $[Co_3(L2O)_4]Cl_2\cdot 5.2H_2O$, $C_{68}H_{76}N_{16}Cl_2Co_3O_{9.2}$, tetragonal, $a = 17.998(1)$ Å, $c = 28.804(3)$ Å, space group $I4_1/a$, $Z = 4$; $[Co(L1O)_2Na(L1O)_2Co][BF_4]\cdot 0.5H_2O\cdot 0.5^iPr_2O\cdot 2MeCN$, $C_{59}H_{44}N_{18}BCo_2F_4NaO_5$, monoclinic, $a = 14.377(3)$ Å, $b = 18.712(2)$ Å, $c = 26.732(2)$ Å, $\beta = 103.30(1)°$, space group $P2_1/c$, $Z = 4$; $[Co_3(L2O)_4][BF_4]_2\cdot 2H_2O\cdot 0.5^iPr_2O$, $C_{35.5}H_{41.5}N_8BCo_{1.5}F_4O_{3.25}$, orthorhombic, $a = 19.076(2)$ Å, $b = 13.872(1)$ Å, $c = 16.363(2)$ Å, space group $P2_12_12_1$, $Z = 4$; $[Co_3(L2O)_4][BF_4]_2\cdot MeCN$, $C_{70}H_{79}N_{17}B_2Co_3F_8O_4$, monoclinic, $a = 22.047(4)$ Å, $b = 16.155(2)$ Å, $c = 21.343(3)$ Å, $\beta = 92.86(1)°$, space group: $C2/c$, $Z = 4$; $[Ni(L1O)_2Co(L1O)_2Ni][BF_4]_2\cdot 2MeCN$, $C_{56}H_{50}N_{18}B_2CoF_8Ni_2O_4$, monoclinic, $a = 40.782(3)$ Å, $b = 16.511(2)$ Å, $c = 19.891(1)$ Å, $\beta = 111.508(6)°$, space group $C2/c$, $Z = 8$; $[Ni(L1O)_2Zn(L1O)_2Ni][BF_4]_2\cdot MeCN$, $C_{54}H_{44}N_8B_2F_8Ni_2O_4Zn$, monoclinic, $a = 12.374(1)$ Å, $b = 26.481(4)$ Å, $c = 18.651(4)$ Å, $\beta = 103.69(1)°$, space group $C2/c$, $Z = 4$; $[Co(L1O)_2Zn(L1O)_2Co][BF_4]_2$, $C_{60}H_{61}N_{17}B_2Co_2F_8O_5Zn$, triclinic, $a = 15.071(2)$ Å, $b = 15.331(2)$ Å, $c = 17.148(2)$ Å, $\alpha = 65.120(7)°$, $\beta = 68.905(8)°$, $\gamma = 71.678(8)°$, space group $P\bar{1}$, $Z = 2$.

Introduction

We have previously described the synthesis and some of the coordination properties of a new class of "heteroscorpionate" ligands (Figure 1) of the general type L_2CX, where L = 3- and/or 5-substituted pyrazole and X = a functionalized donor, i.e., a substituted phenol or thiophenol.[1−5] We have shown that the nature of the metal complexes formed depends on the particular metal involved and the degree of substitution on the pyrazole arms, as well as the ligand-to-metal ratio. By varying the ligand-to-metal ratio, it is possible to prepare not only the mononuclear "sandwich" complexes but also a series of homometallic di- and trinuclear species where, due to the basicity of the coordinated phenols, the octahedrally coordinated "sandwich" complex functions as a ligand for another metal which is tetrahedrally coordinated. The solid-state structures of some of these complexes have already been described.[4] It was noted that the mononuclear complexes could in theory exist as either "cis" or "trans" isomers although only the trans isomer was found in the solid state. Likewise the trinuclear species can also exist as "cis" or "trans" isomers, and in the case of the unsubstituted ligand, crystal structures showed the cis isomer for the Zn^{2+} complex and the trans for the divalent Co, Ni, and Cu analogues.[4] Herein we report the solid-state structures of some new members of this series as well as their isomeric speciation in solution as determined by proton NMR. Using this information, it has been possible to devise a synthetic method for producing heterometallic trinuclear complexes which are of importance for elucidating the magnetic behavior of these octahedral−tetrahedral−octahedral systems.[4] The new heterometallic species, which have been fully characterized including X-ray crystal structures, also provide an interesting experimental

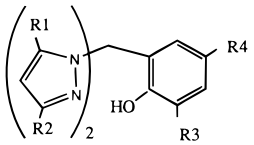

L1OH: R1 = H; R2 = H; R3 = H; R4 = H

L2OH: R1 = Me; R2 = Me; R3 = H; R4 = H

L3OH: R1 = H; R2 = H; R3 = t-butyl; R4 = Me

Figure 1. "Heteroscorpionate" ligands L1OH, L2OH, and L3OH used in this study.

(1) Higgs, T. C.; Carrano, C. J. *Inorg. Chem.* **1997**, *36*, 291.
(2) Higgs, T. C.; Carrano, C. J. *Inorg. Chem.* **1997**, *36*, 298.
(3) Higgs, T. C.; Carrano, C. J. *Inorg. Chim. Acta*, in press.
(4) Higgs, T. C.; Carrano, C. J. *Inorg. Chem.*, in press.
(5) Higgs, T. C.; Ji, D.; Czernuszewicz, R. S.; Matzanke, B. F.; Schunemann, V.; Trautwein, A. X.; Helliwell, M.; Ramirez, W.; Carrano, C. J. *Inorg. Chem.*, in press.

S0020-1669(97)01163-4 CCC: $15.00
Published on Web 03/07/1998

verification for the site preferences (O_h vs T_d) predicted for the first-row divalent transition metal cations on the basis of crystal field stabilization energies.

Experimental Section

All operations were carried out in air unless otherwise stated, and the solvents used were of reagent grade or better (Aldrich Chemical Co.). Microanalyses were performed by the Desert Analytics Laboratory, Tucson, AZ. IR spectra were recorded in KBr disks on a Perkin-Elmer 1600 Series FTIR. Solution electronic spectra were obtained using a Hewlett-Packard 8452A diode array spectrophotometer under the computer control of a Compaq Deskpro 386S with OLIS model 4300 data system diode array spectrophotometry software (On-line Instruments Inc.). ^{1}H NMR spectra were recorded on a 400 MHz Varian INOVA NMR spectrometer at 25 °C unless otherwise noted. Proton spectra (400 MHz) of the paramagnetic complexes of interest were normally acquired using a 100−200 kHz sweep width, an aquisition time of 0.7 s, and a 7 μs pulse width. Typically 32 transients were accumulated, the FID multiplied with 20 Hz line broadening and the transformed spectrum baseline corrected. In some cases a two pulse sequence was used to suppress the diamagnetic resonances from lattice solvents and more clearly reveal peaks from the paramagnetic complexes in the 0−10 ppm area. Ligands (2-hydroxyphenyl)bis-(pyrazolyl)methane, L1OH, and (2-hydroxyphenyl)bis(3′,5′-pyrazolyl)-methane, L2OH, were prepared using literature procedures.[2]

Complex Synthesis. [Co(L2O)$_2$CoCl$_2$], 1. L2OH (0.20 g, 6.757 × 10^{-4} mol) and NaOMe (0.0365 g, 6.757 × 10^{-4} mol) were dissolved in refluxing MeCN (5 mL). Separately $CoCl_2$ (0.0877 g, 6.757 × 10^{-4} mol) was dissolved in hot MeCN (5 mL) forming a dark blue solution. The two solutions were combined, and a white microcrystalline precipitate of NaCl rapidly deposited from the resultant deep blue solution. The reaction mixture was refluxed for 30 min before being filtered hot. The filtrate was then allowed to stand and cool slowly to room temperature overnight, during which time deep blue block crystals deposited from the solution. These were collected, washed with MeCN (2 mL), and dried in vacuo. Yield: 0.125 g (48%). Anal. Calcd for $C_{36}H_{41}N_9Cl_2Co_2O_2$: C, 52.69; H, 5.00; N, 15.37. Found: C, 52.86; H, 5.23; N, 15.24. IR (cm^{-1}): 2984, 2922, 1594, 1559, 1487, 1447, 1380, 1350, 1302, 1267, 1155, 1114, 1042, 986, 902, 873, 788, 760, 695, 579, 545, 478.

[Co$_3$(L2O)$_4$]Cl$_2$·H$_2$O, 2. L2OH (0.50 g, 1.689 × 10^{-3} mol) and NaOMe (0.0913 g, 1.689 × 10^{-3} mol) were dissolved in MeOH (15 mL), and to this solution was added $CoCl_2$ (0.206 g, 1.689 × 10^{-3} mol) forming a deep pink/purple solution which precipitated a blue solid ([Co(L2O)$_2$CoCl$_2$]). Separately a solution of L2OH (0.10 g, 3.38 × 10^{-4} mol) and NaOMe (0.0182 g, 3.38 × 10^{-4} mol) was made up in MeOH (5 mL). This NaL2O solution was carefully "titrated" into the continuously stirred reaction mixture until the majority of the blue solid had redissolved. The reaction mixture was then filtered and the filtrate allowed to stand over a period of days during which time the mother liquor deposited a mass of pink/purple crystals. These crystals were collected by filtration, washed with MeOH (1−2 mL) and Et_2O (5 mL), and dried in vacuo. Yield: 0.32 g (53%). Anal. Calcd for $C_{68}H_{80}N_{16}Cl_2Co_3O_6$: C, 55.75; H, 5.47; N, 15.30. Found: C, 55.45; H, 5.48; N, 15.30. IR (cm^{-1}): 3386, 1594, 1560, 1485, 1447, 1388, 1350, 1317, 1289, 1260, 1154, 1114, 1041, 902, 872, 760, 694, 582, 543, 477.

[Co$_3$(L2O)$_4$][BF$_4$]$_2$·5H$_2$O, 3. Co(BF$_4$)$_2$·6H$_2$O (0.192 g, 5.65 × 10^{-4} mol) was dissolved in MeOH (10 mL) forming a pale purple solution. To this was added NaL2O (0.20 g, 5.65 × 10^{-4} mol), which instantly dissolved forming a pink/purple solution, followed by the rapid precipitation of a microcrystalline pink/purple solid. The reaction mixture was stirred for 20 min at room temperature before the solid was collected by filtration, washed with MeOH (5 mL), and dried in vacuo. Yield: 0.158 g (73%). Anal. Calcd for $C_{68}H_{86}N_{16}B_2Co_3F_8O_9$: C, 50.36; H, 5.31 N, 13.82. Found: C, 50.32; H, 4.70; N, 13.85. IR (cm^{-1}): 3431, 1596, 1560, 1486, 1446, 1388, 1351, 1319, 1290, 1261, 1041, 902, 868, 790, 757, 693, 578, 477.

[Zn$_3$(L2O)$_4$][BF$_4$]$_2$, 4. NaL2O (0.20 g, 5.65 × 10^{-4} mol) was dissolved in MeOH (10 mL). Separately, Zn(BF$_4$)$_2$·6H$_2$O (0.0784 g, 2.26 × 10 × 10^{-4} mol) was dissolved in MeOH (5 mL) and the two solutions combined and stirred at room temperature for 20 min. The reaction mixture was then reduced in volume to approximately 8−10 cm^3 before being cooled to −78 °C in a dry ice/acetone bath until a slight turbidity was observed. The reaction mixture was then allowed to warm to room temperature, during which time a colorless microcrystalline solid was deposited from the mother liquor. This solid was collected by filtration, washed with cold MeOH (2 mL) and Et_2O (5 mL), and dried in vacuo. This material was then dissolved in a small amount of MeCN (3−4 mL) and layered with ^{i}Pr$_2$O (12−14 mL). Over a period of days, small colorless crystals formed. Once a sufficient amount of material had crystallized, the mother liquor was carefully removed by pipet and the crystals were dried in vacuo. Yield: 0.08 g (37%). Anal. Calcd for $C_{68}H_{76}N_{16}B_2F_8O_4Zn_3$: C, 52.66; H, 4.9; N, 14.45. Found: C, 52.58; H, 4.67; N, 14.54. IR (cm^{-1}): 3448, 1596, 1560, 1488, 1447, 1420, 1388, 1351, 1319, 1298, 1260, 1154, 1048, 989, 904, 867, 792, 760, 691, 574, 537, 468.

[Co(L1O)$_2$Na(L1O)$_2$Co][BF$_4$]·H$_2$O, 5. L1OH (0.50 g, 2.083 × 10^{-3} mol) was dissolved in MeOH (10 cm^3), and to this solution was added solid NaOMe (0.113 g, 2.083 × 10^{-3} mol), which quickly dissolved to form a very pale yellow solution. Separately Co(BF$_4$)$_2$·6H$_2$O (0.284 g, 8.332 × 10^{-4} mol) was dissolved in MeOH (5 mL) which was then *slowly* added dropwise to the vigorously stirred solution of NaL1O. As the Co^{2+} was added, the solution changed to a slightly deeper yellow color, then became turbid and precipitated a yellow microcrystalline solid. After completion of the addition, the reaction mixture was stirred for 20 min at room temperature before the solid was collected by filtration, washed with MeOH (5 mL), and dried in vacuo. Yield: 0.47 g (76%). Anal. Calcd for $C_{52}H_{46}N_{16}BCo_2F_4NaO_5$: C, 51.93; H, 3.83; N, 18.64. Found, C, 52.00; H, 3.66; N, 18.66. IR (cm^{-1}): 3133, 1594, 1508, 1482, 1443, 1404, 1326, 1309, 1287, 1252, 1095, 1062, 981, 901, 803, 752, 723, 630, 611, 576, 523.

[Ni(L1O$_2$)Cu(L1O)$_2$Ni][BF$_4$]$_2$, 6. [Ni(L1O)$_2$] (0.40 g, 6.69 × 10^{-4} mol) was suspended in MeCN (10 mL), and to this suspension was added Co(BF$_4$)$_2$·6H$_2$O (0.134 g, 4.01 × 10^{-4} mol), which caused the solution to instantly change to an intense crimson color and the [Ni(L1O)$_2$] to dissolve. The reaction mixture was stirred for 25 min at room temperature before being filtered. The solution was then evaporated to dryness under a reduced pressure yielding a deep crimson microcrystalline solid. This solid was suspended in MeOH (10 mL), vigorously stirred for several minutes, and then cooled to −20 °C (in a freezer) overnight. The solid was then collected by filtration, washed with MeOH (2 mL), and dried in vacuo. Yield: 0.19 g (43%). Anal. Calcd for $C_{52}H_{44}N_{16}B_2CuF_8Ni_2O_4$: C, 44.55; H, 3.86; N, 15.99. Found: C, 44.72; H, 3.33; N, 15.88. IR (cm^{-1}): 3394, 3123, 1596, 1485, 1448, 1408, 1289, 1266, 1206, 1064, 924, 897, 854, 834, 807, 759, 720, 615, 584, 533, 478.

[Ni(L1O$_2$)Co(L1O)$_2$Ni][BF$_4$]$_2$·2H$_2$O, 7. [Ni(L1O)$_2$] (0.20 g, 3.345 × 10^{-4} mol) was suspended in MeCN (10 mL), and to this suspension was added Co(BF$_4$)$_2$·6H$_2$O (0.057 g, 1.673 × 10^{-4} mol), which caused the color of the solution to instantly change to red/purple and the [Ni(L1O)$_2$] to dissolve. The reaction mixture was stirred for 10 min at room temperature before being filtered. The solution was then evaporated to dryness under a reduced pressure yielding a red/purple microcrystalline solid. This solid was suspended in MeOH (5 mL), collected by filtration, washed with more MeOH (2 mL), and dried in vacuo. Yield: 0.17 g (78%). Anal. Calcd for $C_{52}H_{48}N_{16}B_2CoF_8Ni_2O_6$: C, 46.50; H, 3.58; N, 16.69. Found: C, 46.68; H, 3.30; N, 16.69. IR (cm^{-1}): 3396, 3129, 1596, 1570, 1485, 1448, 1406, 1291, 1263, 1066, 898, 856, 834, 805, 755, 717, 632, 615, 576, 537.

[Ni(L1O$_2$)Zn(L1O)$_2$Ni][BF$_4$]$_2$·2H$_2$O, 8. This was prepared as described above using [Ni(L1O)$_2$] (0.20 g, 3.345 × 10^{-4} mol) and Zn(BF$_4$)$_2$·6H$_2$O (0.058 g, 1.673 × 10^{-4} mol). Yield: 0.16 g (73%). Anal. Calcd for $C_{52}H_{48}N_{16}B_2F_8Ni_2O_6Zn$: C, 46.28; H, 3.56; N, 16.61. Found: C, 46.30; H, 3.49; N, 16.63. IR (cm^{-1}): 3404, 3124, 3010, 1596, 1570, 1485, 1448, 1407, 1291, 1262, 1067, 992, 898, 857, 834, 805, 756, 719, 632, 614, 583, 537, 480.

[Co(L1O$_2$)Zn(L1O)$_2$Co][BF$_4$]$_2$·2H$_2$O, 9. This compound was prepared as above using [Ni(L1O)$_2$] (0.20 g, 3.345 × 10^{-4} mol) and Zn(BF$_4$)$_2$·6H$_2$O (0.060 g, 3.345 × 10^{-4} mol). Yield: 0.17 g (77%). Anal. Calcd for $C_{52}H_{48}N_{16}B_2Co_2F_8O_6Zn$: C, 46.26; H, 3.56; N, 16.61.

Found: C, 46.52; H, 3.36; N, 16.46. IR (cm^{-1}): 3414, 3134, 3010, 1596, 1570, 1508, 1487, 1444, 1405, 1289, 1262, 1066, 988, 898, 860, 806, 759, 720, 674, 632, 613, 582, 538, 480.

Crystallography. Crystals of $[Co_2(L2O)_2Cl_2]$·MeCN were grown from a saturated MeCN solution, those of $[Co_3(L2O)_4]Cl_2$·5.2H_2O from a MeOH solution, and those of $[Co(L1O)_2Na(L1O)_2Co][BF_4]$·0.5$H_2O$·0.5^{i}Pr$_2$O·2MeCN by solvent layering of a MeCN solution of the complex with ^{i}Pr$_2$O. Crystals of $[Co_3(L2O)_4][BF_4]_2$·2H_2O·0.5^{i}Pr$_2$O (orthorhombic cell) were grown by vapor diffusion of ^{i}Pr$_2$O into a MeCN solution of the complex, while a monoclinic isomorph, $[Co_3(L2O)_4][BF_4]_2$·MeCN, was obtained from layering an acetonitrile solution with isopropyl ether. $[Ni(L1O)_2Co(L1O)_2Ni][BF_4]_2$·2MeCN, $[Ni(L1O)_2Zn(L1O)_2Ni][BF_4]_2$·MeCN, and $[Co(L1O)_2Zn(L1O)_2Co][BF_4]_2$·MeCN·^{i}Pr$_2$O crystals were all obtained by layering a MeCN solution with ^{i}Pr$_2$O.

All crystals were sealed in thin-walled quartz capillaries to prevent potential loss of lattice solvent to which many of them were prone. The crystals were mounted on a Siemens P4 diffractometer with a sealed-tube Mo X-ray source ($\lambda = 0.710\ 73$ Å) and computer controlled with Siemens XSCANS 2.1 software. Automatic searching, centering, indexing, and least-squares routines were carried out for each crystal with at least 25 reflections in the range $25° \le 2\theta \le 20°$ used to determine the unit cell parameters. During the data collections, the intensities of three representative reflections were measured every 97 reflections, and any decay observed was empirically corrected for by the XSCANS 2.1 software during data processing. The data were also corrected for Lorentz and polarization effects and for $[Co_2(L2O)_2Cl_2]$·MeCN, $[Co_3(L2O)_4]Cl_2$·5.2H_2O, $[Ni(L1O)_2Co(L1O)_2Ni][BF_4]_2$·2MeCN, and $[Co(L1O)_2Zn(L1O)_2Co][BF_4]_2$·MeCN·^{i}Pr$_2$O for X-ray absorption, using a semiempirical correction determined using ψ-scan data. Structure solutions for all these crystals were obtained via direct methods or by use of the Patterson function, and refinement by difference Fourier synthesis was accomplished using the Siemens SHELXTL-PC software package.[6] In the final cycles of refinement the hydrogen atoms in each structure were included in calculated positions using a riding model with fixed isotropic thermal parameters, except for the lattice solvent molecules for which no hydrogen atom positions were calculated. A summary of cell parameters, data collection conditions, and refinement results are presented in Table 1. Details pertinent to the individual refinements are outlined below.

$[Co_2(L2O)_2Cl_2]$·MeCN was solved by direct methods, the asymmetric unit containing one complete $[Co_2(L2O)_2Cl_2]$ molecule and one lattice solvent, MeCN molecule. Bond length and angle data are available as Supporting Information.

The structure of $[Co_3(L2O)_4]Cl_2$·5.2H_2O was solved by direct methods revealing an asymmetric unit containing one-quarter of the $[Co_3(L2O)_4]^{2+}$ cation, with Co1 located on a 4-fold rotoinversion axis and Co2 upon a C_2-rotation axis. Subsequent isotropic refinement (followed by additional anistropic refinement of the Co atoms) of this fragment did not result in the location the expected Cl^- anion (for a fully generated $[Co_3(L2O)_4]^{2+}$ cation there should be 2 Cl^- anions disordered over 4-positions) indicating that the electron density of this atom was "smeared" over the asymmetric unit. As a result the largest two *E*-map electron density peaks were assigned as being due to disordered Cl^- and were assigned occupancies of 0.25 (to give 2 Cl^- anions overall upon full generation of the $[Co_3(L2O)_4]^{2+}$ cation) and refined isotropically. Subsequently the largest *E*-map electron density peaks were assigned as solvent water oxygen atoms, and when these were refined isotropically together with their occupancies, the resulting final *E*-map was quite flat (with the largest remaining peak having an electron density <0.5 e $Å^{-3}$). Detailed bond lengths and angles are available in the Supporting Information while summary values are given in Table 2.

$[Co_3(L2O)_4][BF_4]_2$·2H_2O·0.5^{i}Pr$_2$O (orthorhombic cell) was solved by direct methods, the initial solution indicating that the asymmetric unit contained one-half of a $[Co_3(L2O)_4]^{2+}$ cation with the central Co1 atom of the trinuclear moiety lying upon a crystallographic C_2-axis. Isotropic refinement of this fragment revealed the further presence of a $[BF_4]^-$ anion, one-half of a ^{i}Pr$_2$O lattice solvent molecule (the O3 of

(6) Sheldrick, G. M. *SHELXTL-PC*, version 4.1; Siemens X-ray Analytical Instruments, Inc.: Madison, WI, 1989.

Table 1. Crystallographic Data and Data Collection Parameters for $[Co_2((l2o_2)Cl_2]$·MeCN, $[Co_3((l2o)_4]Cl_2$·5.2H_2O, $[Co(L1O)_2Na(L1O)_2Co][BF_4]$·0.5$H_2O$·0.5^{i}Pr$_2$O·2MeCN, $[Co_3((l2o)_4][BF_4]_2$·2H_2O·0.5^{i}Pr$_2$O, $[Co_3((l2o)_4][BF_4]_2$·MeCN, $[Ni(L1O)_2Co(L1O)_2Ni][BF_4]_2$·2MeCN, $[Ni(L1O)_2Zn(L1O)_2Ni][BF_4]_2$·MeCN, and $[Co(L1O)_2Zn(L1O)_2Co][BF_4]_2$·MeCN·^{i}Pr$_2$O

param	$[Co_2(L2O)_2Cl_2]$	$[Co_3(L2O)_4]Cl_2$	$[Co_2Na(L1O)_4][BF_4]$	$[Co_3(L2O)_4][BF_4]_2$	$[Co_3(L2O)_4][BF_4]_2$	$[Ni_2Co(L1O)_4][BF_4]_2$	$[Ni_2Zn(L1O)_4][BF_4]_2$	$[Co_2Zn(L1O)_4][BF_4]_2$
formula	$C_{36}H_{41}N_9Cl_2Co_2O_2$	$C_{68}H_{76}N_{16}Cl_2Co_3O_{9.2}$	$C_{59}H_{44}N_{18}BCo_2F_4NaO_5$	$C_{35.5}H_{41.5}N_8BCCo_{1.5}F_4O_{3.25}$	$C_{70}H_{79}N_{17}B_2CoF_8O_4$	$C_{56}H_{50}N_{18}B_2CoF_8Ni_2O_4$	$C_{54}H_{44}N_8B_2F_8Ni_2O_4Zn_1$	$C_{60}H_{61}B_2Co_2F_8N_{17}O_5Zn$
space group	$P2_1/c$	$I4_1/a$	$P2_1/c$	$P2_12_12$	$C2/c$	$C2/c$	$C2/c$	$P\bar{1}$
a, Å	10.742(1)	17.998(1)	14.377(3)	19.076(2)	22.047(4)	40.782(3)	12.374(1)	15.071(2)
b, Å	21.387(2)		18.712(2)	13.872(1)	16.155(2)	16.511(2)	26.481(4)	15.331(2)
c, Å	16.890(2)	28.804(3)	26.732(2)	16.363(2)	21.343(3)	19.891(1)	18.651(4)	17.148(2)
α, deg								65.120(7)
β, deg	95.506(8)		103.30(1)		92.86(1)	111.508(6)	103.69(1)	68.905(8)
γ, deg								71.688(8)
V, Å^3	3862.58(84)	9330.8(11)	6998.8(14)	4330.0(8)	7592.2(20)	12461.0(18)	5937.8(13)	3291.0(10)
ρ, g cm^{-3}	1.411	1.077	1.245	1.239	1.376	1.481	1.512	1.470
Z	4	4	4	4	4	8	4	2
fw	820.5	1512.3	1312.8	807.5	1572.9	1389.1	1351.5	1457.1
μ, mm^{-1}	1.041	0.636	0.547	0.640	0.726	0.946	1.114	0.944
R^a	4.23	7.65	6.51	7.58	8.99	6.51	7.07	4.17
$R_w{}^a$	5.25	9.76	7.87	9.06	9.54	7.48	8.18	5.44

^{a} Quantity minimized $\omega w(F_o - F_c)^2$. $R = \sum|F_o - F_c|/\omega F_o$, $R_w = (\omega w(F_o - F_c)^2/\sum(\omega F_o)^2)^{1/2}$.

Table 2. Summary of Significant Structural Parameters for Homo- and Heterometallic Linear Trinuclear Cations of the Form $[M_t(L)_2M_c(L)_2M_t]^{2+}$ (where L = $L1O^-$ or $L2O^-$)

system	M_t	M_c	M_t	mean $O-M_c-O(M_tO_2M_c)$/deg	mean $O-M_t-O$/deg	mean M_c-O/Å	mean M_t-O/Å	mean M_t-O-M_c/deg	mean $M_t\cdots M_c$/Å
$[Co_3(L2O)_4]Cl_2$	Co	Co	Co	82.1	76.3	1.979	2.102	100.8	3.145
$[Co_3(L2O)_4][BF_4]_2$ (monoclinic)	Co	Co	Co	83.0	77.4	1.964	2.081	99.8	3.094
$[Co_3(L2O)_4][BF_4]_2$ (orthorhombic)	Co	Co	Co	82.5	75.7	1.961	2.109	100.9	3.139
$[Ni(L1O)_2Co(L1O)_2Ni][BF_4]_2$	Ni	Co	Ni	83.1	79.0	1.963	2.048	99.0	3.051
$[Ni(L1O)_2Zn(L1O)_2Ni][BF_4]_2$	Ni	Zn	Ni	83.3	79.2	1.958	2.054	98.8	3.035
$[Co(L1O)_2Zn(L1O)_2Co][BF_4]_2$	Co	Zn	Co	83.6	77.4	1.955	2.083	99.5	3.082

this molecule being located upon a C_2-axis), and three partially occupied H_2O molecules (O4, O5, and O6 with occupancies of 0.25, 0.50, and 0.25, respectively). Upon convergence of the initial isotropic refinement, anisotropic refinement was undertaken on all the non-hydrogen atoms except for the B-atom of the $[BF_4]^-$ group and the lattice solvent molecules.

Summary bond length and angles are given in Table 2 with details available in the Supporting Information.

$[Co_3(L2O)_4][BF_4]_2$·MeCN (monoclinic cell) was solved by direct methods. The asymmetric unit contained one-half of a $[Co_3(L2O)_4]^{2+}$ cation, the central Co1 of this trinuclear unit being located on a C_2-rotation. This moiety was refined isotropically which further revealed the presence of a $[BF_4]^-$ group and a lattice MeCN solvent molecule, at 0.5 occupancy, within the asymmetric unit. All the non-hydrogen atoms were refined isotropically and then the Co metal ions, the nitrogen atoms, and the $[BF_4]^-$ group were refined anisotropically. Full atom coordinate, bond length, and angle, and thermal parameter data for this molecule are presented in the Supporting Information.

The structure of $[Co(L1O)_2Na(L1O)_2Co][BF_4]$·$0.5H_2O$·$0.5{}^iPr_2O$·2MeCN was solved by direct methods revealing one complete $[Co(L1O)_2Na(L1O)_2Co]^+$ cation within the asymmetric unit. Subsequent isotropic refinement, followed by anisotropic refinement of the Co and Na atoms of this moiety further revealed the presence of a disordered $[BF_4]^-$ anion, two molecules of lattice MeCN, one H_2O molecule, and one $^iPr_2O$ molecule, both of the latter being at 0.5 occupancy. The $[BF_4]^-$ was disordered with one F-atom occupying two positions (F1A and F1B); the occupancies of these two positions were tied to give an overall value of 1.0 and then refined giving values of 0.6 for F1A and 0.4 for F1B. Upon convergence of this initial, mainly isotropic, refinement the rest of the non-hydrogen atoms were then refined anisotropically with the exception of the lattice solvent atoms and the B-atom of the $[BF_4]^-$ group which were left isotropic. Selected bond length and angle data defining the coordination environments about the one Na and two Co atoms are given in Table 3.

The structure of $[Ni(L1O)_2Co(L1O)_2Ni][BF_4]_2$·2MeCN was solved by direct methods, revealing an asymmetric unit containing a complete $[Ni(L1O)_2Co(L1O)_2Ni]^{2+}$ cation. Initial refinement of this moiety followed by anisotropic refinement of the Ni and Co atoms revealed the additional presence of two disordered $[BF_4]^-$ anions and two lattice MeCN solvent molecules within the asymmetric unit. The two $[BF_4]^-$ anions each contained one F-atom that was disordered over two positions (F1 and F1A for the B1 $[BF_4]^-$ group and F5 and F5A for the B2 $[BF_4]^-$ anion). These two pairs of F-atom positions had their respective occupancies tied to equal an overall value of 1.0, and these were then refined giving values of 0.70 (F1), 0.30 (F1A), 0.75 (F5), and 0.25 (F5A). After the initial isotropic refinement of the contents of the asymmetric unit, all the non-hydrogen atoms were then refined anisotropically. Selected bond length and angle data are summarized in Table 2.

For $[Ni(L1O)_2Zn(L1O)_2Ni][BF_4]_2$·MeCN, during the automatic searching, centering, indexing, and least-squares routines to obtain the unit cell parameters it became obvious that crystals of this complex were twinned with occasional peaks exhibiting a pronounced "doubled" structure. By careful selection of low- and high-angle data, eliminating the twinned peaks, it was possible to elucidate reasonable cell parameters for this crystal and collect data using this orientation matrix. Solution of this structure was accomplished via direct methods, the asymmetric unit containing one-half of a $[Ni(L1O)_2Zn(L1O)_2Ni]^{2+}$ cation, the two Ni and Zn atoms sitting along a C_2-rotation axis (which generates the second half of the cation). Isotropic refinement of this fragment further indicated the presence of a highly disordered $[BF_4]^-$ anion and a lattice MeCN solvent molecule at 0.5 occupancy. The $[BF_4]^-$ group possessed two F-atoms that were disordered over two positions (F3, F3A and F4, F4A). These two pairs of F-atom positions had their respective occupancies tied to equal an overall value of 1.0, and these were then refined giving values of 0.70 (F3), 0.30 (F3A), 0.70 (F4), and 0.30 (F4A). All the non-hydrogen atoms were made anisotropic except for the MeCN solvent molecule and the two lower occupancy, F3A and F4A, F-atoms. Selected bond length and angle data defining the coordination environments about the Ni and Zn atoms are again given in Table 2.

Finally, the structure of $[Co(L1O)_2ZnCo(L1O)_2][BF_4]$·$^iPr_2O$·MeCN was solved by direct methods revealing the complete $[Co(L1O)_2ZnCo(L1O)_2]^+$ cation within the asymmetric unit. Also evident were an acetonitrile and an isopropyl ether of crystallization. One BF_4^- anion was ordered while the other contained one F-atom that was disordered over two positions (F4 and F4a). This pair of F-atom positions had their combined occupancies tied to an overall value of 1.0, and the individual occupancies were then refined to give values of 0.80 (F4) and 0.20 (F4a). All atoms in the structure were refined anisotropically

Table 3. Significant Bond Distances (Å) and Angles (deg) for $[Co(L1O)_2Na(L1O)_2Co][BF_4]$·$0.5H_2O$·$0.5{}^iPr_2O$·2MeCN

Distances with Co1			
Co1−O4	2.017(7)	Co1−O3	2.035(7)
Co1−N11	2.111(10)	Co1−N9	2.161(8)
Co1−N15	2.132(9)	Co1−N13	2.092(8)
Angles with Co1			
O3−Co1−O4	90.5(3)	O4−Co1−N9	89.6(3)
O3−Co1−N9	84.5(3)	O3−Co1−N11	91.8(3)
O4−Co1−N11	173.9(3)	N9−Co1−N11	85.0(3)
O4−Co1−N13	92.9(3)	O3−Co1−N13	93.0(3)
N11−Co1−N13	92.6(4)	N9−Co1−N13	176.4(4)
O3−Co1−N15	176.3(3)	O4−Co1−N15	85.9(3)
N9−Co1−N15	96.6(3)	N11−Co1−N15	91.8(3)
N13−Co1−N15	86.2(3)		
Distances with Co2			
Co2−O1	2.044(7)	Co2−O2	2.008(6)
Co2−N1	2.136(11)	Co2−N3	2.108(9)
Co2−N5	2.129(10)	Co2−N7	2.096(12)
Angles with Co2			
O2−Co2−N1	90.4(3)	O1−Co2−N1	83.7(3)
O1−Co2−N3	92.3(3)	O2−Co2−N3	173.7(4)
N1−Co2−N3	85.5(4)	O2−Co2−N5	86.8(3)
O1−Co2−N5	178.8(3)	N3−Co2−N5	88.9(4)
N1−Co2−N5	96.4(4)	O1−Co2−N7	94.2(2)
O2−Co2−N7	91.6(3)	N1−Co2−N7	177.1(4)
N3−Co2−N7	92.6(4)	N5−Co2−N7	85.7(5)
O1−Co2−O2	92.0(3)		
Distances with Na1			
Na1−O1	2.333(8)	Na1−O2	2.277(8)
Na1−O3	2.342(8)	Na1−O4	2.268(8)
Angles with Na1			
O1−Na1−O3	166.3(3)	O1−Na1−O2	78.4(3)
O1−Na1−O4	109.6(3)	O2−Na1−O3	109.2(3)
O3−Na1−O4	77.3(3)	O2−Na1−O4	118.1(3)
Co−O−Na Angles			
Co1−O4−Na1	93.3(3)	Co2−O1−Na1	89.4(3)
Co1−O3−Na1	90.7(3)	Co2−O2−Na1	91.9(2)

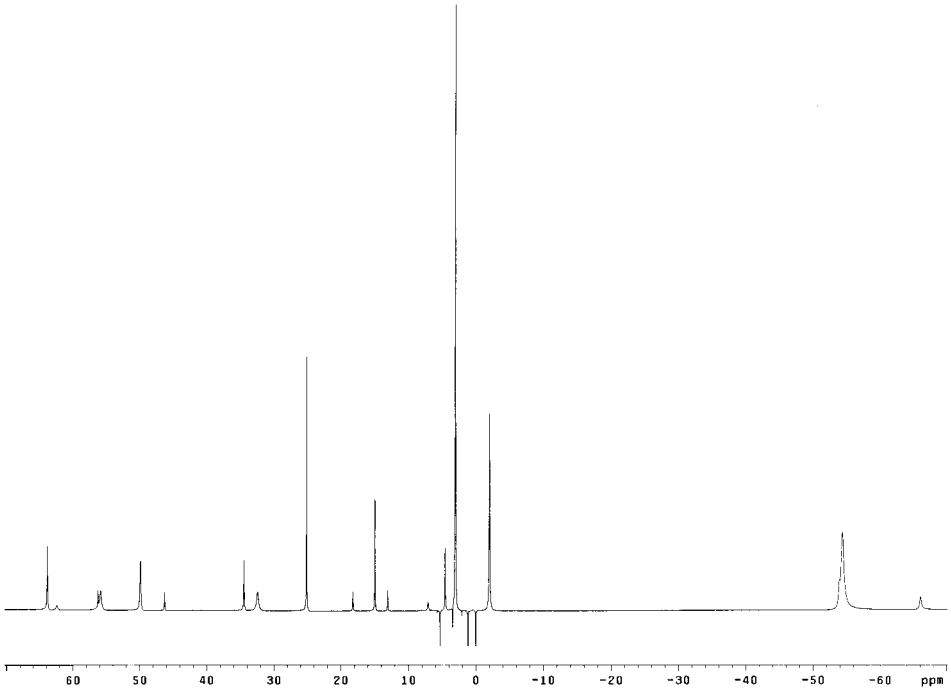

Figure 2. Proton NMR spectra of $(L2O)_2Co$ in CD_2Cl_2 with conditions as decribed in the text.

except the low-occupancy F4a which was left isotropic. Summary bonding parameters are found in Table 2.

Results and Discussion

"Cis−Trans" Isomerization in Monomers of Co^{2+} and Ni^{2+}. In principle, mononuclear "sandwich", i.e. ML_2, complexes of our heteroscorpionate ligands can exist in two isomeric forms, i.e. with the two phenolates cis or trans to each other. We have isolated such complexes for both Ni^{2+} and Co^{2+} with three differently substituted ligands, and in each case, in the solid state, only the "trans" isomer is observed (details of the synthesis and solid-state structures for the unsubstituted and 3,5-dimethylpyrazole derivatives have already been reported,[2] while that for the *tert*-butylmethylphenol will be reported separately[7]). However, in solution the various complexes differ considerably both in the relative stability of the two isomers and in their interconversion rates. In the case of paramagnetic Co^{2+} complexes the cis and trans isomers proved to be easily distinguishable by proton NMR since this ion normally gives rise to relatively sharp but substantially paramagnetically shifted lines due to favorable electronic spin relaxation times.[8] The trans isomer possesses a plane of symmetry rendering the two pyrazole rings of the ligand equivalent, and hence, 8 lines are expected. In the cis isomer the pyrazoles are inequivalent with one being trans to a phenol and the other trans to another pyrazole; thus, 11 lines should be observed. For the *tert*-butyl- and methyl-substituted phenolate ligand L3O (data not shown) only 8 relatively narrow lines are observed in $CDCl_3$ at room temperature indicating that, as in the solid state, only the trans isomer is present in solution. Detailed assignment of these resonances requires more extensive NMR studies which are beyond the scope of this report. However at the present level of sophistication proton NMR still serves to unequivocally "characterize" the geometry (either cis or trans) in solution.

The situation is different for the 3,5-dimethylpyrazole-substituted ligand L2O (Figure 2). Here 19 lines can be seen corresponding to an admixture of both the cis and trans isomers with the ratio of trans to cis approximately 3:1. The fact that this ratio is maintained even when crystals, shown by X-ray diffraction to contain only the trans isomer, are dissolved demonstrates that in solution the two isomers are in equilibrium with each other but in relatively slow exchange on the NMR time scale.

When the unsubstituted ligand, L1O, is used the situation is even more complex. In this case only 6 very broad lines (several hundred Hz) are seen at 25 °C. The small number and extreme broadness of the lines suggests that an equilibrium is set up which has a time constant on the order of the NMR time scale. Since we were limited on the high-temperature side by the volatility of the dichloromethane-d_2 solvent, we attempted to cool the solution to slow the exchange process. Indeed as the temperature was lowered the peaks began to shift and broaden out still further with a coalescence point near 0 °C. As the temperature was lowered further the spectrum sharpened up and by −40 °C 19 relatively sharp peaks could be observed, consistent with a mixture of both the cis and the trans isomers. The ratio of trans to cis in this case was ca. 1:1. Unfortunately the temperature dependence of the peak positions and line widths could not be analyzed to extract the rate constant for the interconversion between the isomers since those parameters were also affected in a temperature-dependent manner by the paramagnetism of the cobalt (Curie law). The following overall features are clear, however: (1) As one moves from the unsubstituted through the 3,5-dimethylpyrazole to the *tert*-butylmethylphenol ligands, the rate of cis/trans interconversion slows down markedly. (2) As the degree of substitution on the ligand increases, so does the relative stability of the trans isomer over the cis. The increasing kinetic inertness of the substituted complexes is reasonable from a steric viewpoint and has been well documented for the topologically similar tris(pyrazolyl)-borates.[9] The increasing stability of the trans isomer with increasing bulk on the ligand also likely has a steric origin. The fact that with the unsubstituted ligand only the trans complex

(7) Higgs, T. C.; Carrano, C. J. Manuscript in preparation.
(8) *NMR of Parmagnetic Molecules; Principles and Applications*; La Mar, G. N., Horrocks, W., Eds.; Academic Press: New York, 1973.
(9) Mohan, M.; Holmes, S. M.; Butcher, R. J.; Jasinski, J. P.; Carrano, C. J. *Inorg. Chem*. **1992**, *31*, 2029.

is isolated in the solid state, even though both are present in approximately equal amounts in solution, is likely the result of its being either the least soluble isomer or to more favorable crystal packing forces.

Homometallic Dimers. Synthesis and structural characterization of the homometallic dimer NiL_2NiCl_2, where L = L2O, have already been reported.[1] The solid-state structure of the cobalt analogue, $[Co(L2O)_2CoCl_2]\cdot MeCN$, reveals nothing unexpected; hence, details are relegated to the Supporting Information.

In solution Co dimers of the form $L_2CoCoCl_2$ show even more dramatically paramagnetically shifted proton NMR spectra than the monomers due to the presence of two high-spin cobalt(II) centers in the molecule. While the monomer spectrum is completely contained within the −60 to +60 ppm range, the dimer is spread out over the range from −120 to +120 ppm (data not shown). Once again we make no attempt to assign all 11 peaks (the dimer can only have the cis geometry about the octahedral L_2Co unit in order for it to function as a bidentate ligand for the tetrahedral cobalt) but rather use the NMR simply as a qualitative signiture of the dimer's presence in solution. The dimer of the 3,5-dimethyl-substituted ligand appears to undergo some dissociation in dichloromethane solution at 25 °C as evidenced by small NMR peaks associated with the monomer, i.e.

$$L_2CoCoCl_2 \rightarrow L_2Co + CoCl_2$$

Isomerization in Homometallic Trimers. Homometallic trimers of the type L_2MMML_2, where L = L1O and M = Cu^{2+}, Zn^{2+}, Ni^{2+}, and Co^{2+}, have already been reported by us.[4] In that report we noted that two different isomers of such trimers are possible and that the Zn derivative adopted the "cis" structure while the other metals displayed the "trans" form. To avoid confusion with the "cis" and "trans" forms of the L_2M complexes we hereafter adopt the "syn" and "anti" nomenclature to describe the isomers of the trimetallics. In an effort to determine what factors might be important in which isomer was isolated, we have synthesized and characterized both in the solid state and in solution several more of these trimers with Zn and Co as metals using different solvents and counterions.

X-ray structures for the Cl^- salt and two isomorphs of the BF_4^- salt of the Co trimer have been obtained. The only significant structural difference between the monoclinic and orthorhombic crystal forms of $[Co_3(L2O)_4][BF_4]_2$ are their two $M_tO_2M_c$ dihedral angles, ω, with values 57.6 and 67.8°, respectively. We attribute this difference to crystal packing effects since the lattice solvation of $[Co_3(L2O)_4][BF_4]_2\cdot MeCN$ (monoclinic) and $[Co_3(L2O)_4][BF_4]_2\cdot 2H_2O\cdot 0.5^iPr_2O$ (orthorhombic)) and thus the packing in the two cells are inequivalent. The chloride and tetrafloroborate salts of the $[Co_3(L2O)_4]^+$ cation however differ significantly in that the former adopts the syn geometry while the latter displays the anti (Figure 3). Thus while solvation seems to have little effect on isomer preference, the counterion clearly is important. A summary of their bonding parameters is given in Table 2.

In solution the Co linear trimers follow the same trend established with the monomers and dimers; i.e., the proton NMR shows even greater shifts and covers the range from −240 to +130 ppm. More complete electronic and magnetic characterization of these interesting mutinuclear paramagnetic complexes in solution will hopefully be forthcoming, but again proton NMR is a useful qualitative tool for determining solution speciation. There are 11 major lines in the spectrum of the tetrafloroborate salt of the 3,5-dimethyl derivative, consistent

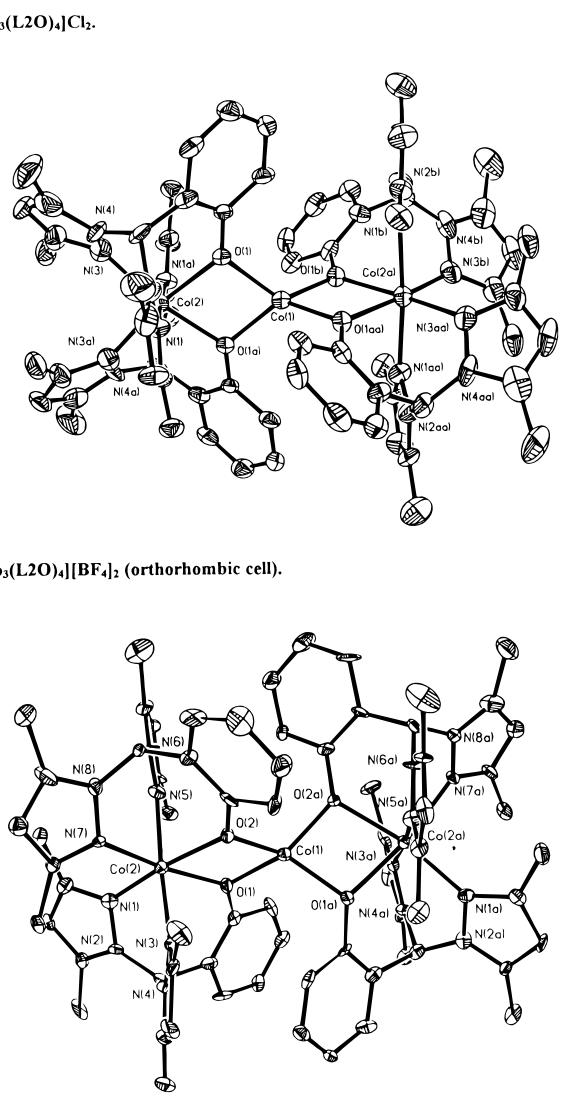

Figure 3. ORTEP views of the *syn*-$[Co_3(L2O)_4]^{2+}$ cation with 30% thermal ellipsoids and selected atomic labeling as the chloride salt (top) and the *anti*-$[Co_3(L2O)_4]^{2+}$ cation as the tetrafloroborate salt (bottom).

with the required cis geometry of the terminal L_2Co units, but an additional set of 11 minor resonances are also clearly observed (Figure 4a). These minor resonances are not due to either the monomer or dimer but rather to the other isomeric form. Since in the solid state the BF_4^- salt of the cobalt linear trimer with the 3,5-dimethyl ligand adopts the anti configuration, we assign this isomer to the major resonances. The minor resonances are then assigned to the syn isomer, which is also present in solution. The anti/syn ratio is about 9:1 in MeCN and is not strongly solvent dependent, being nearly the same in CH_2Cl_2 and MeOH. The counterion however has a major effect on the relative stability of the two isomers both in solution and in the solid state. In the solid state the chloride salt adopts exclusively the syn isomer rather than the anti seen with the BF_4^-. In solution the syn isomer predominates as well, although only slightly, with a syn/anti ratio of 1.1:1 (Figure 4b). For the BF_4^- salt of the linear trimer with the unsubstituted ligand in MeCN the anti isomer predominates (as in the solid state); however, the ratio of anti/syn in solution is only about 4.8:1 rather than the 9:1 found for the 3,5-dimethyl ligand complex.

The differences in isomeric composition for the cobalt linear trimers between the Cl^- and BF_4^- salts prompted us to investigate the effects of chloride addition to solutions of the BF_4^- salt. Addition of chloride ion to a dichloromethane or

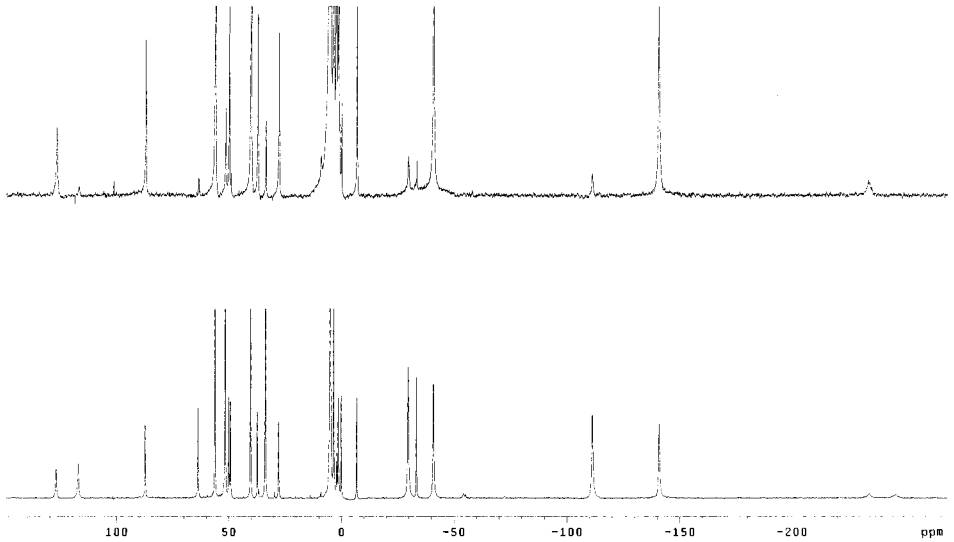

Figure 4. NMR spectra of the tetrafloroborate salt of the $[Co_3(L2O)_4]^{2+}$ cation (top) and of the chloride salt of the same cation (bottom) in CD_3OD with conditions as decribed in the text.

acteonitrile solution of the tetrafloroborate salt of the 3,5-dimethyl Co linear trimer does not induce isomerization but rather produces a mixture of the trimer, dimer, and monomer as determined by proton NMR. The ratio of dimer to monomer produced is 1:1 indicating that the reaction occurs stoichiometrically, i.e.

$$L_2CoCoCoL_2 + 2Cl^- \rightarrow L_2CoCoCl_2 + L_2Co$$

The same process occurs without addition of exogenous chloride upon dissolution of the chloride salt of the linear trimer in a suitable solvent. Thus the solution absorption spectra of $[Co_3(L2O)_4]Cl_2$ obtained in MeOH and MeCN are completely different from each other in contrast to the solvent insensitivity of the tetrafloroborate salt. A MeOH solution of $[Co_3(L2O)_4]Cl_2$ is pink in color, similar to that of the solid, crystallographically characterized material, whereas a MeCN solution is blue in color and the electronic spectrum of the solution is identical to that of $[Co_2(L2O)_2Cl_2]$. In addition, allowing the MeCN solution to stand results in a yellow material being deposited which proved to be that of the monomer *trans*-$[Co(L2O)_2]$. These observations indicate that in MeCN solution the chloride salt of the trinuclear cation, $[Co_3(L2O)_4]^{2+}$, is unstable cleaving to give monomeric $[Co(L2O)_2]$ and dinuclear $[Co_2(L2O)_2Cl_2]$. Overall these results indicate that chloride is a better ligand for the tetrahedral M(II) center than is the L_2M unit. The cleavage of the trimer into monomer and dimer can also be effected by other anionic nucliophiles such as cyanide. Running the cleavage reaction in acetonitrile, a solvent in which the reactant trimer is very soluble and the product L_2M monomer only sparingly soluble, effectively drives the reaction to completion. Although we have not yet exploited this reaction to any great extent, it is clear that a wide variety of octahedral−tetrahedral homometallic dimers could be synthesized by this route.

Trinuclear Heterometallics. The observation that both the cis and trans isomers of the mononuclear species L_2M were present in solution as determined by proton NMR suggested a method for preparing heterometallic species of the type $L_2MM'ML_2$ since the cis isomer can function as a ligand for a new central metal M′. Thus addition of a mono- or divalent cation to a slurry of a monomer in acetonitrile (a solvent in which the monomer is only sparingly soluble) caused the instant dissolution of the solid monomer and the formation of a heterometallic trimer. The added cation clearly sequesters the cis form of the monomer as the linear trimer which is soluble in acetonitrile thus effectively driving the equilibrium to completion despite the fact that the cis form was always the minor isomer in the starting monomer. The CoNaCo, NiCoNi, NiZnNi, and CoZnCo heterometallic trimers have all been synthesized and characterized in the solid state by X-ray crystallography while several others have only been examined in solution by proton NMR.

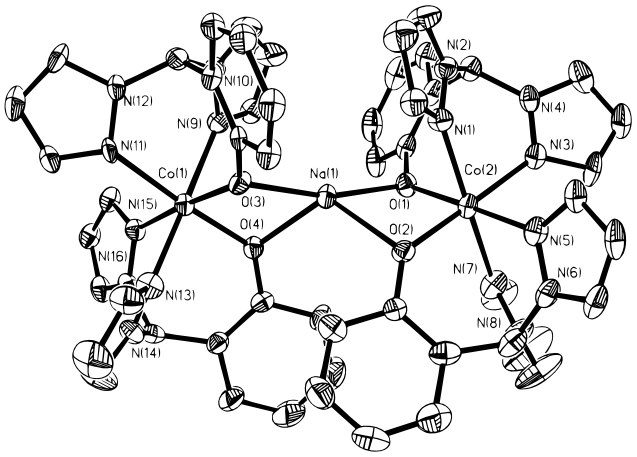

Figure 5. ORTEP view of the *anti*-$[Co(L1O)_2Na(L1O)_2Co]^+$ cation with selected atom labeling.

An ORTEP view of the structure of the $[Co(L1O)_2Na(L1O)_2Co]^+$ cation is shown in Figure 5. The trinuclear cation contains two terminal Co^{2+} atoms and one central Na^+ atom in a near linear array with a Co−Na−Co angle of 172.7(2)°. The two terminal Co^{2+} atoms are each coordinated to two tridentate N_2O donor $L1O^-$ ligands with their stereochemistries best described as slightly distorted octahedral. The phenolate-*O* ligands are oriented cis to each other and bridge to a single Na^+ atom which is O_4-coordinated. The Na stereochemistry is highly distorted and can be described as being either very distorted tetrahedral or trigonal bipyramidal with an equatorial ligand "removed" since the O3−Na1−O1 bond angle (166.3(3)°) is close to the trans-axial value for this geometry (180°) and the next largest angle, O2−Na1−O4 (118.1(3)°), possesses a value close to that expected for a equatorially situated pair of ligands in this geometry. It is surprising that another small

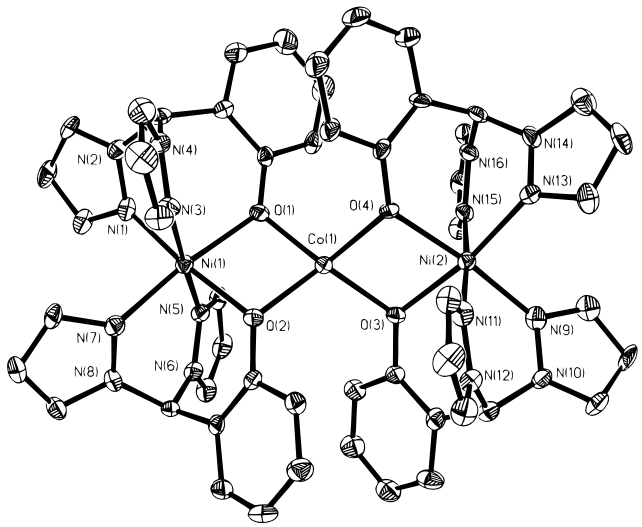

Figure 6. ORTEP view of the *anti*-$[Ni(L1O)_2Co(L1O)_2Ni]^{2+}$ cation with 30% thermal ellipsoids and selected atom labeling.

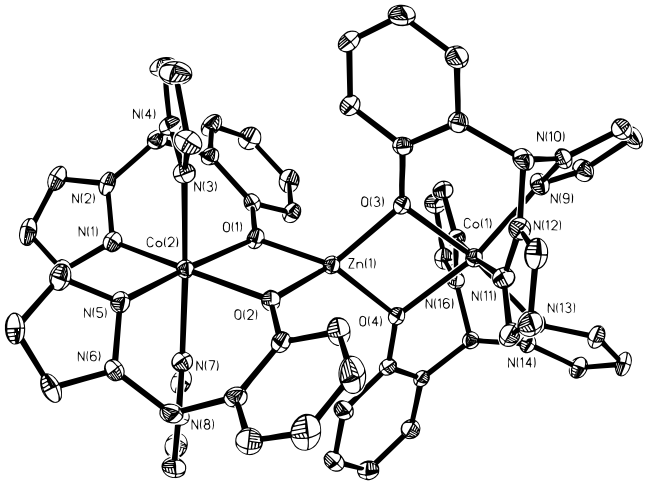

Figure 7. ORTEP view of the *syn*-$[Co(L1O)_2Zn(L1O)_2Co]^{2+}$ cation with 30% thermal ellipsoids and selected atom labeling.

exogenous ligand, perhaps a H_2O molecule, does not occupy the "open" equatorial site of this geometry since there is a precedent for this in the trinuclear cation $[Mn_3(L1O)_4(MeCN)]^{2+}$, which has a 5-coordinate, central, trigonal bipyramidal Mn^{2+} atom with an MeCN equatorial exogenous ligand.[4] The stereochemistries of the two terminal Co^{2+} atoms are quite regular octahedral with only one "cis" L−Co−L bond angle having a greater than 5° distortion from the "ideal" 90° value. The terminal Co−N (average, 2.121 Å) and Co−O (average, 2.026 Å) bond lengths compare favorably with those of other octahedral $L1O^-$- and $L2O^-$-coordinated Co^{2+} sites. The Co−O−Na1 angles mediate Co1···Na1 and Co2···Na1 separations of 3.120 and 3.085 Å respectively.

Since each of the other heterometallics are quite similar to each other and their homometallic counterparts, we simply summarize the bonding data in Table 2 and provide only a general description of the structures. ORTEP's for the *anti*-NiCoNi and *syn*-CoZnCo derivatives are illustrative of the entire series (Figures 6 and 7). The $[M_t(L)_2M_c(L)_2M_t]^{2+}$ cations all contain three transition metal ions in a linear or near-linear array ($M_t-M_c-M_t$ angles range from 177.2 to 180.0°). The two terminal M_t^{2+} atoms of these cations are coordinated by two tridentate, "scorpionate" ligands ($L1O^-$ or $L2O^-$) and are thus 6-coordinate possessing psuedooctahedral stereochemistries. The phenolate-*O* ligand donors within these distorted octahedral coordination environments are orientated cis to each other and bridge to a single, third metal ion, M_c^{2+}, the central metal ions of these trinuclear cations. The M_c^{2+} metal ions are thus coordinated by four bridging phenolate oxygens, with an overall distorted tetrahedral geometry. Dihedral angles, ω, range from 58° for the NiCoNi complex to 67° for NiZnNi species. The ω values for all the crystallographically characterized trinuclear cations are summarized in Table 4. The individual bond angles defining the 4-coordinate M_c^{2+} stereochemistries show considerable distortions from the "ideal" tetrahedral value with the most significant deviation in the $O-M_c-O$ angles of the $M_tO_2M_c$ bridging moieties which are highly compressed as a result of the formation of the strained four-membered chelate $M_tO_2M_c$ rings. The terminal, 6-coordinate, M_t^{2+} atoms all have only slightly distorted octahedral stereochemistries. The terminal M_t-O_{Ph} bond lengths are invariably longer than those of the central metal ions, M_c-O_{Ph}, due to the differing stereochemistries of these cations. The mean M_t-O-M_c bridging angles range from about 99 to 101° and mediate mean $M_t\cdots M_c$ separations of 3.035−3.145 Å (Table 2).

Table 4. Illustration of the Relationship between the Magnitude of the Dihedral Angle, ω, of the Central Metal Ion of Homo- and Heterometallic Trinuclear Cations of the Type $[M(L)_2N(L)_2M]^{2+}$ (Where L = $L1O^-$ or $L2O^-$) and the Isomeric (Syn or Anti) Form of the Cation

system	central metal	dihedral angle, ω (deg)	isomeric form
$[Cu_3(L1O)_4][BF_4]_2\cdot 2MeCN$	Cu^{II}	46.8	anti
$[Co_3(L1O)_4][BF_4]_2\cdot MeCN$	Co^{II}	61.2	anti
$[Ni_3(L1O)_4][ClO_4]_2\cdot MeCN\cdot 0.5H_2O$	Ni^{II}	60.4	anti
$[Zn_3(L1O)_4][BF_4]_2\cdot H_2O$	Zn^{II}	79.9	syn
$[Co_3(L2O)_4]Cl_2\cdot 5.2H_2O$	Co^{II}	90.0	syn
$[Co_3(L2O)_4][BF_4]_2\cdot 2H_2O\cdot 0.5{}^iPr_2O$[a]	Co^{II}	67.8	anti
$[Co_3(L2O)_4][BF_4]_2\cdot MeCN$[b]	Co^{II}	57.6	anti
$[Ni(L1O)_2Co(L1O)_2Ni][BF_4]_2\cdot 2MeCN$	Co^{II}	58.2	anti
$[Ni(L1O)_2Zn(L1O)_2Ni][BF_4]_2\cdot MeCN$	Zn^{II}	67.0	anti
$[Co(L1O)_2Zn(L1O)_2Co][BF_4]_2\cdot MeCN$	Zn^{II}	84.0	syn

[a] Orthorhombic cell. [b] Monoclinic cell.

As in the homometallic trimers, both syn and anti isomers are observed for the heterometallic cations as well (Table 4). An interesting observation from Table 4 is that all the syn isomers in this series of compounds have an ω value of 80−90°, whereas the anti isomers have ω values in the range 57.6−67.8° (average 63 ± 5°), except for the all Cu trimer. The Cu(II) trimer is anomalous due to the pronounced preference of this Jahn−Teller distorted ion to adopt a square planar rather tetrahedral geometry.[4]

Table 5 summarizes the solution electronic spectral data for the new heterometallic compounds along with some of the homometallic complexes for comparison. Putative band assignments made in Table 5 are based primarily on the energy of the absorption and its intensity since d−d bands in tetrahedral crystal fields are typically more intense (by about 10×) than those in octahedral environments due to the absence of a center of symmetry in the former.[12] Thus in these di- and trinuclear systems which contain M^{2+} atoms in both tetrahedral and

(10) (a) Addison, A. W.; Rao, T. N.; Reedijk, J.; van Rijn, J.; Verschoor, G. C. *J. Chem. Soc., Dalton Trans.* **1984**, 1349. (b). Zoeteman, M.; Bouwman, E.; de Graff, R. A. G.; Driessen, W. L.; Reedijk, J.; Zanello, P. *Inorg. Chem.* **1990**, *29*, 3487.
(11) Nicholls, D. *Comprehensive Inorganic Chemistry*; Bailar, J. C., Emeleus, H. J., Nyholm, R., Trotman-Dickenson, A. F., Eds.; Pergamon Press: Oxford, U.K., 1973; Vol. 3, pp 1152−1159.
(12) Brink, J. M.; Rose, R. A.; Holz, R. C. *Inorg. Chem.* **1996**, *35*, 2878.

Table 5. Summary of Electronic Spectral Results

complex	electronic band positions, nm (cm^{-1})	extinction coeff, ϵ	proposed band assgn
$[Co_2(L2O)_2Cl_2]$ (in CH_2Cl_2)	354 (28 250), sh	510	charge transfer
	478 (20 920)	44	d−d ("O_h")
	536 (18 660), sh	127	d−d ("T_d")
	564 (17 730)	387	d−d ("T_d")
	608 (16 450), w sh	184	d−d ("T_d")
	646 (15 480)	388	d−d ("T_d")
$[Co_3(L2O)_4][BF_4]_2$ (in MeCN)	342 (29 340), sh	1005	charge transfer
	474 (21 100)	223	d−d ("T_d")
	552 (18 115)	155	d−d ("T_d")
	584 (17 120)	213	d−d ("T_d")
$[Co_3(L2O)_4]Cl_2$ (in MeOH)	344 (29 070) sh	990	charge transfer
	482 (20 750), w sh	100	d−d ("T_d")
	520 (19 230)	280	d−d ("T_d")
	556 (17 985)	357	d−d ("T_d")
	570 (17 545)	370	d−d ("T_d")
	584 (17 120)	355	d−d ("T_d")
	608 (16 450)	117	d−d ("T_d")
$[Co_3(L2O)_4]Cl_2$ (in MeCN)	354 (28 250), sh	1770	charge transfer
	480 (20 830)	36	d−d ("O_h")
	534 (18 725), sh	110	d−d ("T_d")
	564 (17 730)	351	d−d ("T_d")
	610 (16 390)	179	d−d ("T_d")
	646 (15 480)	345	d−d ("T_d")
$[Ni(L1O)_2Cu(L1O)_2Ni][BF_4]_2$ (in MeCN)	330 (30 300), sh	2570	charge transfer
	456 (21 930), w sh	3490	$O_{ph} \rightarrow Cu^{II}$ CT
	504 (19 840)	4010	$O_{ph} \rightarrow Cu^{II}$ CT
$[Ni(L1O)_2Co(L1O)_2Ni][BF_4]_2$ (in MeCN)	340 (29 410), sh	525	charge transfer
	474 (21 100)	174	d−d ("T_d" Co^{II})
	550 (18 180)	135	d−d ("T_d" Co^{II})
	566 (17 670)	154	d−d ("T_d" Co^{II})
	584 (17 120)	203	d−d ("T_d" Co^{II})
	598 (16 720), sh	143	d−d ("T_d" Co^{II})
$[Ni(L1O)_2Zn(L1O)_2Ni][BF_4]_2$ (in MeCN)	340 (29 410), sh	102	charge transfer
	548 (18 250)	15	d−d ("O_h" Ni^{II})
	768 (13 020), w sh	11	d−d ("O_h" Ni^{II})
	>820 (12 200)	17	d−d ("O_h" Ni^{II})
$[Co(L1O)_2Zn(L1O)_2Co][BF_4]_2$ (in MeCN)	466 (21 460)	41	d−d ("O_h" Co^{II})
	516 (19 380), w sh	22	d−d ("O_h" Co^{II})
	580 (17 240), sh	6.5	d−d ("O_h" Co^{II})

octahedral coordination environments the electronic spectra in the visible region are dominated by the tetrahedral electronic transitions. Two exceptions to this observation are the heterometallic trinuclear cations, $[Co(L1O)_2Zn(L1O)_2Co][BF_4]_2$ and $[Ni(L1O)_2Zn(L1O)_2Ni][BF_4]_2$, since the central "tetrahedral" M^{2+} atom in these is d^{10} Zn^{2+}, which has no d−d transitions. Thus the electronic spectra of these two systems display only the d−d absorptions of the terminal Co^{2+} and Ni^{2+} atoms which are in octahedral coordination environments and are similar to those of "sandwich" complexes $[Co(L1O)_2]$ and $[Ni(L1O)_2]$ previously reported.[1,2] One other notable exception to the above generalization is the spectrum of $[Ni(L1O)_2Cu(L1O)_2Ni][BF_4]_2$, whose two overlapping visible absorption bands are too intense to be d−d in origin and are thus assigned as being due to $O_{Ph} \rightarrow Cu^{II}$ charge-transfer (CT) transitions. This observation helps to elucidate the relative contributions of the terminal and central Cu^{2+} atoms to the electronic spectrum of the homometallic $[Cu_3(L1O)_4]^{2+}$. This cation is also deep crimson in color resulting from two overlapping $O_{Ph} \rightarrow Cu^{II}$ CT bands in the visible region (452 nm (22 030 cm^{-1}), $\epsilon = 3856$, and 512 nm (19530 cm^{-1}), shoulder, $\epsilon = 3044$). The absorption spectra of the homo- and heterometallic derivatives are somewhat different in shape, but the energies and intensities are very similar. This implies that $O_{Ph} \rightarrow Cu^{II}$ CT transitions to the *central* Cu^{2+} atom in the homometallic $[Cu_3(L1O)_4]^{2+}$ cation make the most important contribution to the two CT overlapping bands observed in the visible region of the electronic spectrum of this system.[3]

Proton NMR spectroscopy was used to determine unequivocally that solutions of the heterometallic trimers maintain their integrity in solution and are not simply statistical mixtures of the corresponding homometallics. As an example, Figure 8 shows the NMR spectrum of the all Cu and all Ni homometallic trimers prepared with the $L1O^-$ ligand along with that of the NiCuNi heterometallic. The spectrum of the latter is clearly not a superposition of $^2/_3$ Ni trimer and $^1/_3$ copper trimer. Interestingly while paramagnetic Ni(II) and Co(II) have long been known to be nuclei amenable to proton NMR, copper complexes have generally not been thought to be so unless they are coupled to favorable ions. However, recent reports indicate that magnetically coupled Cu dinuclear complexes can give rise to sharp NMR spectra even when the coupling is far too weak to generate a diamagnetic ground state.[12,13] The trinuclear homometallic Cu complex reported here also displays a rather sharp NMR spectrum with line widths generally less than 100 Hz. This phenomena is thought to be due to a modulation of the zero field splitting (ZFS) of the $S = 1$ state which can occur via molecular rotation, internal motions, or magnetic interactions in coupled systems.[13] Complexes such as this may be useful in understanding NMR spectra in polynuclear copper enzymes.

"Site Preferences" of First-Row Transition Metal Dications. Despite the successful exploitation of the aforementioned synthetic scheme, not all desired heterometallic species can be synthesized by this route due to the apparent site preference of particular metal ions for the central tetrahedral environment vs the terminal octahedral one. This "site selectivity" was first

(13) Murthy, N. N.; Karlin, K. D.; Bertini, I.; Luchinat, C. *J. Am. Chem. Soc.* **1997**, *119*, 2156.

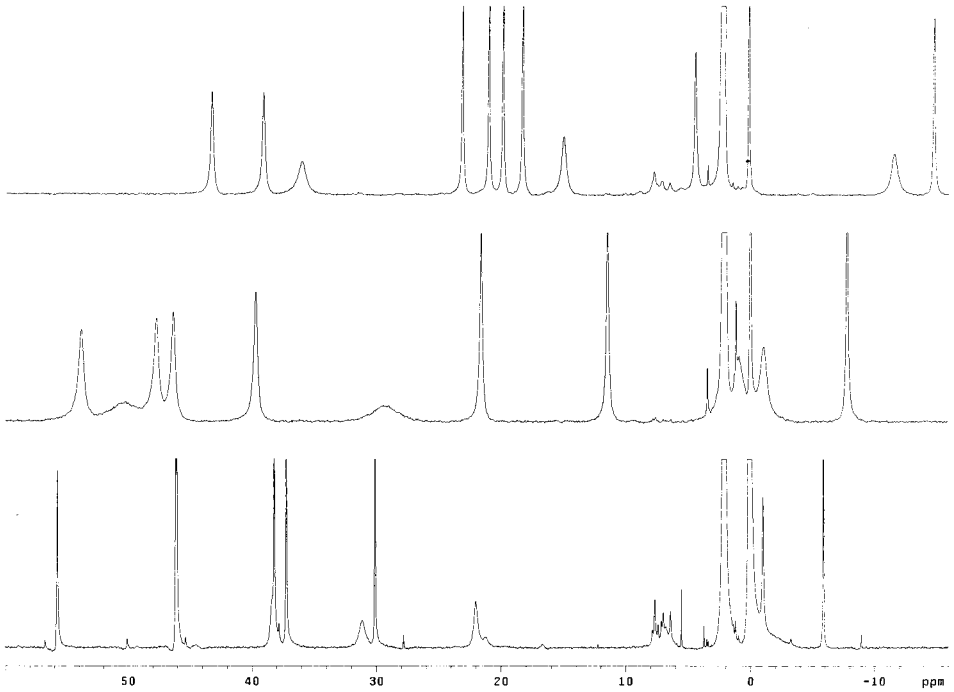

Figure 8. NMR spectra of the $Cu(L1O)_2Cu(L1O)_2Cu$ (top), $Ni(L1O)_2Cu(L1O)_2Ni$ (middle), and $Ni(L1O)_2Ni(L1O)_2Ni$ (bottom) trimers in CD_3CN with conditions as decribed in the text.

made obvious by the electronic spectrum of the material formed from the reaction of $[Co(L1O)_2]$ and 0.5 $Ni(ClO_4)_2 \cdot 6H_2O$. This was expected to produce the CoNiCo trimer with Ni(II) in the central position. However, the material isolated from this reaction had a pink/purple color remarkably similar to that of $[Ni(L1O)_2CoNi(L1O)_2][BF_4]_2$ indicating that a Co^{2+} atom occupied the central position of the trinuclear cation. Comparison of the band intensities to those of the $[Ni(L1O)_2CoNi(L1O)_2]^{2+}$ cation (Table 5) clearly indicated that complete central $\leftrightarrow$ terminal site exchange had occurred between the Ni^{2+} (from the $Ni(ClO_4)_2 \cdot 6H_2O$) and one of the $[Co(L1O)_2]$ "sandwich" complexes during formation of the trinuclear heterometallic cation to give the NiCoCo species. Additional studies, confirmed by X-ray crystallography, allowed the derivation of a "site preference" order for tetrahedral versus octahedral sites with the metals Zn^{2+}, Cu^{2+}, Co^{2+}, and Ni^2.

Highest				*Lowest*
Tetrahedral				*Tetrahedral*
Affinity				*Affinity*
Zn^{2+}	> Co^{2+}	≈ Cu^{2+}	>	Ni^{2+}
Lowest				*Highest*
Octahedral				*Octahedral*
Affinity				*Affinity*

The "site preferences" determined experimentally by this approach can be compared to those expected from simple crystal stabilization energy (CFSE) arguments.[14] The order predicted from the latter is Zn > Co ≈ Cu > Ni, i.e., precisely the same. Although the latter order has been well-known for a very long time, there has been little experimental verification of it.

(14) Cotton, F. A., Wilkinson, G. *Advanced Inorganic Chemistry*, 4th ed.; John Wiley and Sons: New York, 1980; pp 686−7.

Conclusions

The following represent the basic conclusions of this work: (1) Mononuclear "sandwich" complexes of Co(II) with the heteroscorpionate ligands L1−3, which are found only as the trans isomers in the solid state, exist as an equilibrium mixture of both cis and trans isomers in solution. (2) We can make use of this solution equilibrium for the rational synthesis of heterometallic trimers using the concept of "complexes as ligands" and that these heterometallic trimers exist as discrete species both in the solid state and in solution. (3) The synthesis of only certain of the possible heterometallic trimers provides an experimental verification to the octahedral vs tetrahedral site preferences of the first row divalent metals. (4) Homometallic trimers react with halide to produce dimer and monomer in solution but not in the solid state. (5) Homometallic trimers which are found as one or the other of "syn" and "anti" isomers in the solid state exist in solution as a mixture of both.

Acknowledgment. This work was supported by Grant AI-1157 from the Robert A. Welch Foundation, the ACS/PRF, and Grant SF-93−12 from the Dreyfus foundation. NSF Program Grants USE-9151286 and CHE-9601574 are gratefully acknowledged for partial support of the X-ray diffraction and NMR facilities, respectively, at Southwest Texas State University.

Supporting Information Available: Complete listings of atomic positions, bond lengths and angles, isotropic and anisotropic thermal parameters, hydrogen atom coordinates, and data collection and crystal parameters and ORTEP diagrams with complete atomic labeling for **1**−**3**, **5**, and **7**−**9** (86 pages). Ordering information is given on any current masthead page.

IC9711630